

# Capture of Manufacturing Uncertainty in Turbine Blades through Probabilistic Techniques

Nikita Thakur<sup>\*</sup>, Andy Keane<sup>†</sup> and Prasanth B. Nair<sup>‡</sup>

Computational Engineering and Design Group, School of Engineering Sciences, University of Southampton, Southampton, SO17 1BJ, UK.

Efficient designing of the turbine blades is critical to the performance of an aircraft engine. An area of significant research interest is the capture of manufacturing uncertainty in the shapes of these turbine blades. The available data used for estimation of this manufacturing uncertainty inevitably contains the effects of measurement error/noise. In the present work, we propose the application of Principal Component Analysis (PCA) for de-noising the measurement data and quantifying the underlying manufacturing uncertainty. Once the PCA is performed, a method for dimensionality reduction has been proposed which utilizes prior information available on the variance of measurement error for different measurement types. Numerical studies indicate that approximately 82% of the variation in the measurements from their design values is accounted for by the manufacturing uncertainty, while the remaining 18% variation is filtered out as measurement error.

## Nomenclature

<b>C</b>	= covariance matrix
<b>m</b>	= number of measurement locations
<b>n</b>	= number of samples
<b>V</b>	= matrix of eigenvectors
<b>D</b>	= diagonal matrix
$\sigma$	= standard deviation
<b>p</b>	= total number of repeated trials
<b>q</b>	= number of samples for repeated measurements
<b>o</b>	= number of operators
<b>t</b>	= number of repeated measurements by each operator
<b>r</b>	= rank of a matrix
<b>e</b>	= measurement error matrix
<b>a</b>	= measurement location true thickness value matrix
<b>k</b>	= number of principal components
<b>d</b>	= dimensionality obtained from PCA

## Subscripts and Superscripts

<b>T</b>	= matrix transpose
<b>i</b>	= row number

---

Communicating Author: nikita.thakur@soton.ac.uk

<sup>\*</sup>PhD Research Student, CEDG, School of Engineering Sciences.

<sup>†</sup> Professor and Head of Department, CEDG, School of Engineering Sciences.

<sup>‡</sup> Senior Lecturer, CEDG, School of Engineering Sciences.

## I. Introduction

**T**URBINE blades are critical to the performance of an aircraft engine. Identification and quantification of the various types of manufacturing uncertainties in the process of turbine blade manufacture has become a field of research that is claiming increased attention from leading aircraft engine manufacturing companies. "With the introduction of new market paradigms like *Power By The Hour* and *TotalCare* contracts, the engine manufacturers have undertaken the responsibility for providing overall lifetime support to the engine, from the time the engine is delivered to the customer until the engine goes out of service"<sup>[1-3]</sup>. Therefore, characterization and quantification of these manufacturing uncertainties is an important issue in the aircraft engine manufacturing industry due to the effect of these uncertainties on the overall efficiency, performance and life of the engine. At present, not much literature is available on the kind of manufacturing uncertainties that can arise in the final shape of the turbine blades.

In the present work, we consider cooled intermediate pressure (IP) turbine blades which thus have both external and internal design features. In the discussions that follow, knowledge of the sources of manufacturing uncertainties is based on first-hand experience at the Precision Casting Facility (PCF), Rolls Royce plc., Derby. Regular discussions have also been held with manufacturing and design engineers.

Manufacturing of IP turbine blades involves processes such as casting, grinding and polishing, all of which can contribute to shape variation in the blade from its design value. Casting in itself is a very complicated process involving a series of steps and procedures, e.g. designing and manufacturing the moulds, pouring in the hot molten metal, cooling of the casts, and, extraction of blades from moulds. In addition, certain less controllable parameters like temperature, pressure and humidity of the surroundings also add to these uncertainties. Therefore, identification of the nature and sources of manufacturing uncertainty and then the quantification of this manufacturing uncertainty is a significant task. Various experimental methods and techniques, both destructive and non-destructive, are available for quantification of this uncertainty.

One of the destructive techniques is slicing up the sample blades and making internal and external measurements on the blade slices. However, the implementation of this technique depends on the number of blades available for cutting up into slices which may be very expensive to the high cost of production of each blade. Besides, the technology and procedure used for cutting up the blades has to be carefully selected in order to obtain slices with smooth cut-up surfaces that could be used for precise measurements. Also, the dimensions measured for comparison with the design values need to be selected and registered with great care.

One form of a non-destructive technique is to experimentally obtain 3-D scans of the blades and then compare these scans with the designed blade shapes. This process involves highly powered X-ray micro-Computed Tomography (CT) scanners for the high density nickel alloy blades. Such high-powered micro-CT scanners are not easily available and obtaining 3-D scans on the turbine blades with good resolution is a very expensive and time-consuming process. Another non-destructive technique is physically making measurements on the surfaces of the manufactured blades and comparing these measurements with the design values. This is a complicated process due to the complex shape of the blade. Moreover, it gives us no idea of the internal shape variations in the blade, especially for the air-cooled and film-cooled blades which have cooling passages inside them.

Another non-destructive technique, which is being used successfully during the manufacturing process, is making ultrasonic measurements on the blade. This technique uses ultrasonic beams to measure the wall thickness of the blade at various cross-sections and at various points across these cross-sections to record the final shape of the manufactured blade. Besides ultrasonic measurements of wall thicknesses, the other non-destructive evaluation techniques that are currently in use for this purpose are impulse-video-thermography<sup>[5]</sup>, X-ray tomography<sup>[6]</sup> and eddy current technique<sup>[7]</sup>. Ultrasonic wall thickness measurement data can easily be corrupted by errors introduced during the measurement process. Various factors are responsible for introducing measurement errors in the blade thickness measurements e.g. error in calibration of the ultrasonic device, error in orientation of the blade when the objective is to align it perpendicular to the ultrasonic head, error due to the measured surface being out of view, human error, etc. Therefore, it becomes desirable to filter out any error/noise from the measured data to get the final shape of the blade that would represent the actual manufactured blade.

Principal Component Analysis (PCA) is one of the statistical techniques widely employed in de-noising measurement data. PCA is used in various fields like electrocardiogram (ECG) data compression in biomedicine<sup>[8]</sup>, electrical impedance tomography (EIT) in imaging techniques<sup>[9]</sup>, face recognition<sup>[10, 11]</sup>, gene expression analysis in bioinformatics<sup>[12]</sup>, oceanography<sup>[13, 14]</sup>, climatology<sup>[15]</sup>, geophysics<sup>[16, 17]</sup>, geology<sup>[18]</sup>, astronomy<sup>[19, 20]</sup>, shape prediction of femoral heads from partial information<sup>[21]</sup>, reconstruction of human body shapes from range scans in Computer Graphics<sup>[22]</sup> etc. Lately, more complicated forms of PCA have been developed and demonstrated on varying sets of data. Smidl and Quinn<sup>[23]</sup> proposed Bayesian principal component analysis and demonstrated the advantages of orthogonal variational PCA (OVPCA) on scintigraphic dynamic image sequence of kidneys. Tipping

and Bishop <sup>[4]</sup> demonstrated the advantages of Probabilistic Principal Component Analysis (PPCA) by applying the technique on a set of *Tobamovirus* data (a genus that contains viruses that infect plants). Hagan, Roble, Russell and Mlynaczak <sup>[17]</sup> made use of Complex Principal Component Analysis (CPCA) on satellite data for planetary wave and tidal analysis in the middle atmosphere.

The objective of this paper is to demonstrate the application of PCA in separation of measurement variability from measured turbine blade thickness data to obtain the expected actual thicknesses of the manufactured blades that include the effects of manufacturing uncertainty. This paper also proposes an approach to dimensionality reduction after PCA has been performed on the blade thickness data. The proposed approach to dimensionality reduction finds application only when prior information on the measurement error is available. The variance of the measurement error at each measurement position is used as the threshold for cut-off to decide upon the number of principal components (PCs) to be retained.

The flow of discussion in this paper is as follows. In Section II we give an introduction to PCA in terms of its mathematical formulation. In Section III, various techniques that may be used for dimensionality analysis are presented and the proposed approach to dimensionality reduction has been discussed in detail. Section IV discusses the application of PCA and the dimensionality reduction techniques to the measured turbine blade data. Section V discusses the concluding remarks and is followed by acknowledgements and references.

## II. Introduction to PCA

Principal Component Analysis is a non-parametric method of extracting relevant information from complicated datasets <sup>[24]</sup>. “It is a way of identifying patterns in data, and expressing the data in such a way as to highlight their similarities and differences” <sup>[11]</sup>. Let  $\mathbf{X}$  be an  $m \times n$  matrix, where  $m$  is the number of measurement types and  $n$  is the number of samples. Let  $\mathbf{Y}$  be another  $m \times n$  matrix related by a linear transformation  $\mathbf{P}$ . If  $\mathbf{X}$  is the original recorded dataset and  $\mathbf{Y}$  is a re-representation of that dataset, we can apply a linear transformation to  $\mathbf{X}$  such that,

$$\mathbf{P}\mathbf{X} = \mathbf{Y}. \quad (1)$$

Equation (1) represents a change of *basis* such that  $\mathbf{P}$  is a matrix that transforms  $\mathbf{X}$  into  $\mathbf{Y}$ . The goal of PCA is to find the orthonormal matrix  $\mathbf{P}$  where  $\mathbf{Y} = \mathbf{P}\mathbf{X}$  such that the covariance matrix of  $\mathbf{Y}$ , namely  $\mathbf{C}_Y \equiv \frac{1}{n-1} \mathbf{Y}\mathbf{Y}^T$ , is diagonalized. The rows of  $\mathbf{P}$  are the principal components of  $\mathbf{X}$ . We begin by rewriting  $\mathbf{C}_Y$  in terms of our variable of choice  $\mathbf{P}$ .

$$\mathbf{C}_Y = \frac{1}{n-1} (\mathbf{P}\mathbf{X})(\mathbf{P}\mathbf{X})^T = \frac{1}{n-1} \mathbf{P}\mathbf{X}\mathbf{X}^T\mathbf{P}^T = \frac{1}{n-1} \mathbf{P}(\mathbf{X}\mathbf{X}^T)\mathbf{P}^T, \quad (2)$$

$$\mathbf{C}_Y = \frac{1}{n-1} \mathbf{P}\mathbf{A}\mathbf{P}^T, \quad (3)$$

where,

$$\mathbf{A} \equiv \mathbf{X}\mathbf{X}^T. \quad (4)$$

In equation (4),  $\mathbf{A}$  is a *symmetric* matrix which is diagonalized by an orthogonal matrix of its eigenvectors such that:

$$\mathbf{A} = \mathbf{V}\mathbf{D}\mathbf{V}^T, \quad (5)$$

where  $\mathbf{D}$  is a diagonal matrix and  $\mathbf{V}$  is a matrix of eigenvectors of  $\mathbf{A}$  arranged as columns.

The matrix  $\mathbf{A}$  has  $r \leq m$  orthonormal eigenvectors where  $r$  is the rank of the matrix. The rank of  $\mathbf{A}$  is less than  $m$  when  $\mathbf{A}$  is *degenerate* or all data occupy a sub-space of dimension  $r \leq m$ . Maintaining the constraint of orthogonality, this situation can be remedied by selecting  $(m - r)$  additional orthonormal vectors to “fill up” the matrix  $\mathbf{V}$ . These additional vectors do not affect the final solution because the variances associated with these directions are zero.

We select the matrix  $\mathbf{P}$  to be a matrix where each row  $\mathbf{p}_i$  is an eigenvector of  $\mathbf{XX}^T$ . By employing this selection,  $\mathbf{P} \equiv \mathbf{V}^T$ . Substituting into equation (5), we find  $\mathbf{A} = \mathbf{P}^T \mathbf{D} \mathbf{P}$ . Also, we know that the inverse of an orthogonal matrix is its transpose, i.e., for our case  $\mathbf{P}^T = \mathbf{P}^{-1}$ . Evaluating  $\mathbf{C}_Y$  from these two relations, we get:

$$\mathbf{C}_Y = \frac{1}{n-1} \mathbf{P} \mathbf{A} \mathbf{P}^T = \frac{1}{n-1} \mathbf{P} (\mathbf{P}^T \mathbf{D} \mathbf{P}) \mathbf{P}^T = \frac{1}{n-1} (\mathbf{P} \mathbf{P}^T) \mathbf{D} (\mathbf{P} \mathbf{P}^T) = \frac{1}{n-1} (\mathbf{P} \mathbf{P}^{-1}) \mathbf{D} (\mathbf{P} \mathbf{P}^{-1}), \quad (6)$$

$$\mathbf{C}_Y = \frac{1}{n-1} \mathbf{D}. \quad (7)$$

From equation (7), it is evident that the choice of  $\mathbf{P}$  diagonalizes  $\mathbf{C}_Y$ . For a more elaborate description of the theoretical and computational aspects of PCA, the reader is referred to the works by Smith, Jolliffe, Mandel and others <sup>[11, 12, 24-27]</sup>.

### III. Dimensionality Reduction

Once the PCA has been performed, the next issue is choosing the number of Principal Components (PCs) to be retained in order to account for most of the variation in  $\mathbf{X}$  <sup>[27, 28]</sup>. Numerous techniques for dimensionality reduction are available in the literature <sup>[27, 29, 30]</sup>. Many readymade packages in MATLAB are also available which perform dimensionality reduction for a given dataset <sup>[30]</sup>. Some of the techniques which are proposed in the literature are, – 1) selecting a cumulative percentage of total variation such that the selected PCs contribute say 80% or 90% of the total variation <sup>[27]</sup>, 2) *Kaiser's rule* which retains only those PCs whose variances exceed 1 <sup>[27]</sup>, 3) *Scree Graph* <sup>[12, 27]</sup> and the *Log-Eigenvalue Diagram* <sup>[27]</sup>, 4) *Bayesian Model selection* <sup>[28]</sup> etc. A detailed description of these techniques can be found in the works from Jolliffe <sup>[27]</sup> and Minka <sup>[28]</sup>. Other dimensionality reduction techniques for which readymade packages are available in MATLAB are *Correlation dimension estimator*, *Nearest neighbour estimator*, *Maximum likelihood estimator*, *Eigenvalue-based estimator*, *Packing numbers estimator* and *Geodesic minimum spanning tree (GMST) estimator*. Further information on these techniques is available in *An Introduction to Dimensionality Reduction Using Matlab* by Maaten <sup>[30]</sup>. This paper discusses essential details of the two techniques, namely, *Cumulative Percentage of Total Variation* and *The Scree Graph*, since they have been used for validating the results obtained from the application of the proposed dimensionality reduction technique to the measurement dataset.

#### A. Cumulative Percentage of Total Variation

Let us assume that the number of PCs to be retained after PCA has been performed is represented by  $d$ . This technique proposes a criterion for dimensionality reduction such that a cumulative percentage of the total variation accounted for by the first  $d$  PCs is calculated. The number  $d$  is selected such that it accounts for anything between 70% to 90% of the total variation, depending upon the details of the particular dataset being analysed. The cumulative percentage of the total variation accounted for by the first  $d$  PCs may be mathematically represented as below:

$$\text{Cumulative percentage} = 100 \sum_{k=1}^d ev_k / \sum_{k=1}^m ev_k, \quad (8)$$

where,  $ev_k$  represents the  $k^{\text{th}}$  eigenvalue <sup>[27]</sup>.

#### B. The Scree Graph

The *scree* graph proposes dimensionality reduction through a graphical observation of the  $ev_k$  vs.  $k$  plot. The dimensionality  $d$  is selected equal to the value of  $k$  such that the slopes of lines joining the plotted points are ‘steep’ to the left of  $k$  and ‘shallow’ to the right of  $k$  <sup>[27]</sup>.

#### C. Dimensionality reduction using prior information on Measurement Error

The techniques discussed above are very useful when there is no prior knowledge of the noise that needs to be filtered out of the measurement data. However, if we have information available on the noise that is to be removed

from the target input matrix  $\mathbf{X}$ , it is more desirable to use this knowledge for aiding the selection of minimum number of PCs that should be retained.

Due to the availability of data on the measurement error introduced for various measurement types, in the present work, we use this information as the threshold for cut-off when selecting the number of PCs to be retained. Here, information on the measurement error is available in the form of repeated trials of the same experiment on the same sample by  $o$  different operators, where each operator repeats each trial on the same sample  $t$  times. This is done for  $q$  different randomly selected samples. The measurement noise information is converted into a data matrix  $\mathbf{N}$  such that each row is populated with the measurements taken on the same measurement position and each column contains the measurements from a particular trial. For each sample,  $\mathbf{N}$  can be represented as a  $m \times p$  matrix where  $m$  represents the number of measurement types and  $p = o \times t$ . The variance of each row of  $\mathbf{N}$  (say  $\mathbf{n}_i$ , where  $i$  is the number of rows) can be represented as the sum of the variance of actual value of the measurement type (say  $\mathbf{a}_i$ ) and variance due to the measurement error (say  $\mathbf{e}_i$ ),

$$\sigma^2(\mathbf{n}_i) = \sigma^2(\mathbf{a}_i) + \sigma^2(\mathbf{e}_i). \quad (9)$$

The actual value of the same measurement type for repeated measurements on the same sample is constant. Thus,  $\sigma^2(\mathbf{a}_i) = 0$ . Substituting this in equation (9) we get,

$$\sigma^2(\mathbf{n}_i) = \sigma^2(\mathbf{e}_i). \quad (10)$$

Therefore, the variance of each row in the data matrix  $\mathbf{N}$  represents the variance of the measurement error. Similarly, these variances can be calculated for  $q$  different samples. The variances calculated for each of these samples for  $m$  different measurement types could be consolidated into one  $m \times q$  variance matrix. The mean of each row of the variance matrix would finally result in  $m$  different values, one each for  $m$  different measurement types, which may then be used as the threshold for cut-off while selecting the number of PCs to be retained.

#### IV. Numerical Studies

Wall thickness measurements were taken through ultrasonic measurement devices on a set of 1050 randomly selected IP air-cooled turbine blades. This measurement data was made available by the Precision Casting Facility (PCF), Rolls Royce plc., Derby. The thicknesses were measured across three cross-sections (Tip, Mid and Root of the blade) and each section was measured at 6 different locations (pressure side Leading Edge (LE), pressure side center, pressure side Trailing Edge (TE), suction side Trailing Edge, suction side center and suction side Leading Edge). **Fig. 1** shows the measurement locations across a typical cross-section. The locations 1-6 marked in **Fig. 1** were selected such that the minimum thicknesses across each section were recorded. Minimum thicknesses across each section of the blade become important during fatigue failure tests, and lifting and stress analysis.

Out of this 1050 blade dataset, data for 77 blades manufactured on the same day was identified and separated to nullify the uncertainty effects introduced due to changes in the surrounding temperature and humidity levels. These two datasets comprising 77 blades and 1050 blades respectively, were analysed in order to observe and compare the relative drifts in thickness values from one measurement location to another for the 18 different measurement locations. This deviation from nominal was plotted for the two datasets in the form of scatter plots across the 3 cross-sections (Tip, Mid and Root) such that:

$$\text{Deviation from nominal} = \text{Nominal Thickness} - \text{Measured Thickness.} \quad (11)$$

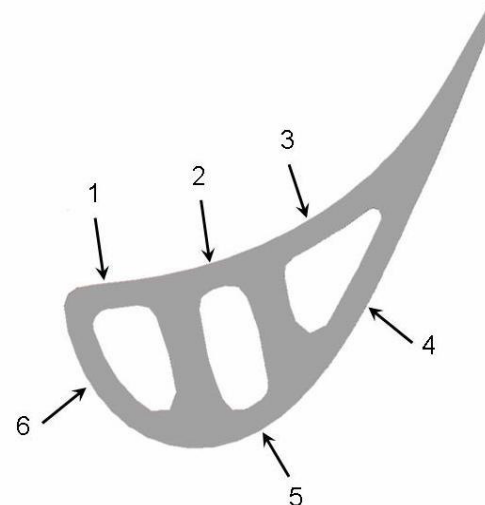


**Fig. 1 Measurement locations across typical cross-section.**

The resultant scatter plots obtained at the Tip-section for the 77 and 1050 blade datasets are shown in **Fig. 2** and **Fig. 3** respectively. Similar plots were also constructed for the Mid and Root-sections. It was observed that for both the datasets, the drifts in mean measurement values from nominal thicknesses across the six measurement locations at Tip-section followed a similar trend. This is apparent from a comparison of **Fig. 2** with **Fig. 3**. Similar trends were also observed for the Mid and Root-sections. This lead to the conclusion that the variation in surrounding temperature and humidity levels did not affect the relative deviation from nominal in blade wall thickness values at the eighteen measurement locations. The entire 1050 blade data could therefore be used directly for a further statistical analysis of the manufacturing uncertainty and measurement variability.

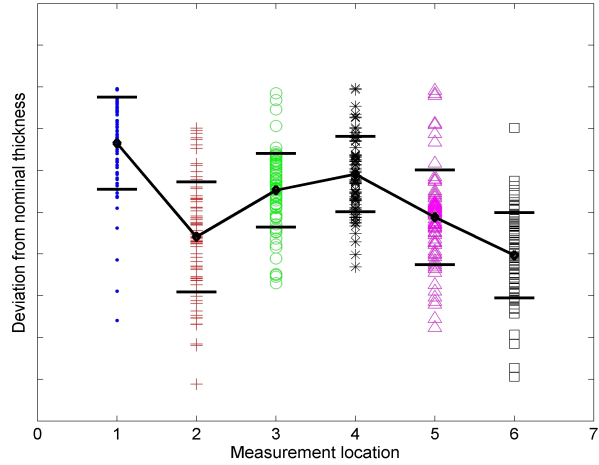


**Fig. 2 Deviation from nominal vs. measurement location at TIP section for 77 blade dataset.**

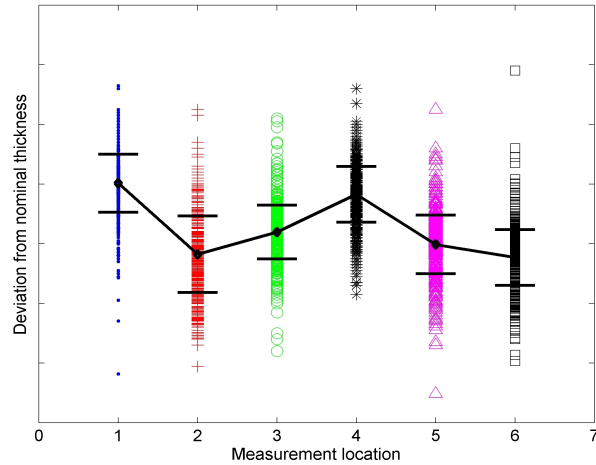


**Fig. 3 Deviation from nominal vs. measurement location at TIP section for 1050 blade dataset.**

The measurement data on the 1050 blades was represented in the form of a matrix  $\mathbf{X}$  where  $m = 18$  and  $n = 1050$  such that rows 1-6 represented the measurements taken on the Tip-section, rows 7-12 represented the measurements taken on the Mid-section and rows 13-18 represented the measurements taken on the Root-section. A PCA was performed on this input data matrix  $\mathbf{X}$ . The resultant plot of the eigenvalues versus number of modes obtained from the application of PCA to the measurement dataset is shown in **Fig. 4**.

Applying the Scree Graph method of dimensionality reduction to the plot in **Fig. 4**, it is observed that for  $k = 5$  the slopes of the lines formed by plotting the points to the left of  $k$  are steeper relative to the slopes on the right of  $k$ . Hence, for the present case, the value of  $d$  may be taken equal to 5. The point  $k = 3$  may also be considered, however it is observed that the slope of the line joining  $k = 4$  and  $k = 5$  becomes steeper again, hence  $d = 5$  seems to be a better choice in this case.

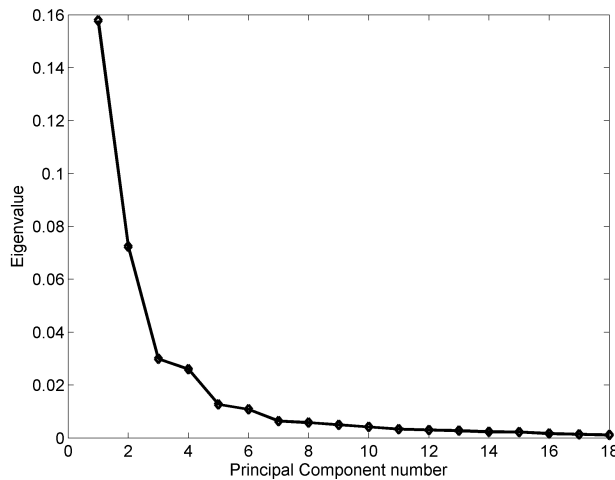


**Fig. 4 Plot of Eigenvalues vs. Principal Component number for the 1050 blade dataset.**

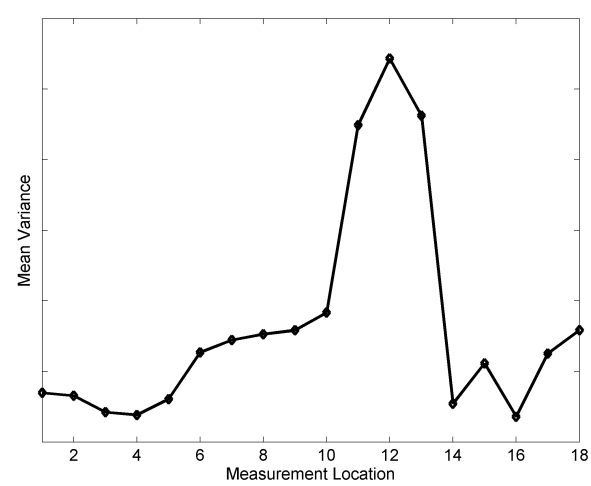


**Fig. 5 Plot of mean variance vs. measurement location on the blade.**

Now, looking at the *Cumulative Percentage of Total Variation* method of dimensionality reduction and keeping 80% of the total variation as the threshold for cut-off, it is observed that:

- a) for  $k = 3$ , cumulative percentage = 74.56%.
- b) for  $k = 4$ , cumulative percentage = 82.02%.
- c) for  $k = 5$ , cumulative percentage = 85.66%.

Observing the values of the cumulative energy content for each of the cases above,  $k = 4$  seems to be the closest possible match to our threshold criterion. Hence, this methodology results in a dimensionality,  $d = 4$ .

The dimensionality analysis using the already existing dimensionality reduction techniques shows that most of the variance is accounted for by the first  $d = 4/d = 5$  modes and the remaining  $18 - d$  modes may be representing random error/noise. This suggests that by using PCA, the shape of the manufactured blades may be reconstructed using the first  $d$  modes and the remaining  $18 - d$  modes would result in the measurement variability.

Following this analysis, the technique proposed for dimensionality reduction using prior information available on the measurement error, as discussed in section III, was applied on the measurement dataset. Information on measurement error was made available to us by a specially designed experiment conducted at PCF, Rolls Royce plc., Derby. Ultrasonic wall thickness measurements were made for a randomly selected sample of 11 IP turbine blades, such that each set of 18 measurements were repeated on the same blade by three randomly selected operators, with each operator repeating the 18 set of measurements four times on the same blade. Since the operators were randomly selected, this data included human error in the measurements. These measurements were taken on different days and at different times of the day thus including the effects of any changes in the day to day temperature, pressure and humidity levels of the surroundings. The random selection of the 11 blades accounted for any other indistinguishable random errors being introduced into the blade shape during the manufacturing process. With this set of 12 trials each on 11 blades, and 18 measurements being taken on each blade, the variances in measurements at the 18 measurement locations were calculated for each blade separately using equation (10). The overall mean of the variances at each location for the 11 blades was then calculated as explained in Section III. The resultant plot of the mean variances vs. measurement location is shown in **Fig. 5**.

It can be observed in **Fig. 5** that the values of variance are maximum at positions 11, 12 and 13 which denote the Mid suction-side center, Mid suction-side LE and Root pressure-side LE, possibly due to the large curvature at these positions. Also, it was observed that the measurement variability at the Tip and Root-sections was lower than that at the Mid-section. A possible reason for this could be difficulty in holding the Mid-section perpendicular to the ultrasonic beam head due to non-firm clamping of the blade. Non-firm clamping increases the possibility of left and right deviations of the blade from the markings on the Mid-section across which measurements are to be taken. A point worth noticing is that the magnitude of the variances across the 18 measurement locations is relatively very small as compared to the magnitude of the actual wall thickness measurements, which are approximately 10-20 times of the maximum value of standard deviation observed for these variances. This may indicate that the measurement variability being introduced by the operators is relatively very small and the operators are well trained.

These values of measurement error variances at the 18 measurement locations were used as threshold for cut-off while deciding upon the number of PCs that were to be retained for reconstruction of the manufactured blades. The value of number of PCs ( $k$ ) was varied between 1-18 such that if the variance of the reconstruction error was less than the threshold value, the  $k$  was reduced and if the variance of the reconstruction error was more than the threshold value, the  $k$  was increased. For the present case, the reconstruction error is defined as:

$$\text{Reconstruction Error} = \text{Original Blade thickness} - \text{Reconstructed Blade Thickness.} \quad (12)$$

This comparison becomes easier when plotted. The plot obtained from PCA which shows a continuous decrease in variance of reconstruction error as the number of PCs are increased is shown in **Fig. 6**. The solid line represents the variances used for dimensionality reduction. The dashed lines represent the variances plotted for reconstruction error as  $k$  increases from 1 to 18. It is observed clearly that the variance in reconstruction error at each measurement position decays with increase in  $k$  till it finally becomes zero when  $k = 18$ . This implies that it is possible to reconstruct the entire input data matrix without losing any information when the number of PCs is selected equal to the number of measurement types. A closer look at the plot in **Fig. 6** revealed that the variance plot obtained for  $k = 4$  resulted in the best possible match to the threshold criterion. The variance plot obtained for  $k = 4$  has been clearly highlighted in **Fig. 6** with a bold dashed line. Hence, the proposed dimensionality reduction criterion resulted in a dimensionality,  $d = 4$ . It is observed that this value of dimensionality matches perfectly with the results obtained from the application of *Cumulative Percentage of Total Variation* technique and is very close to the results observed from the *Scree Graph* technique. It may be concluded therefore, that the proposed dimensionality reduction criterion

is capturing approximately 82% of the variation as manufacturing uncertainty and filtering out the remaining 18% variation as measurement variability.

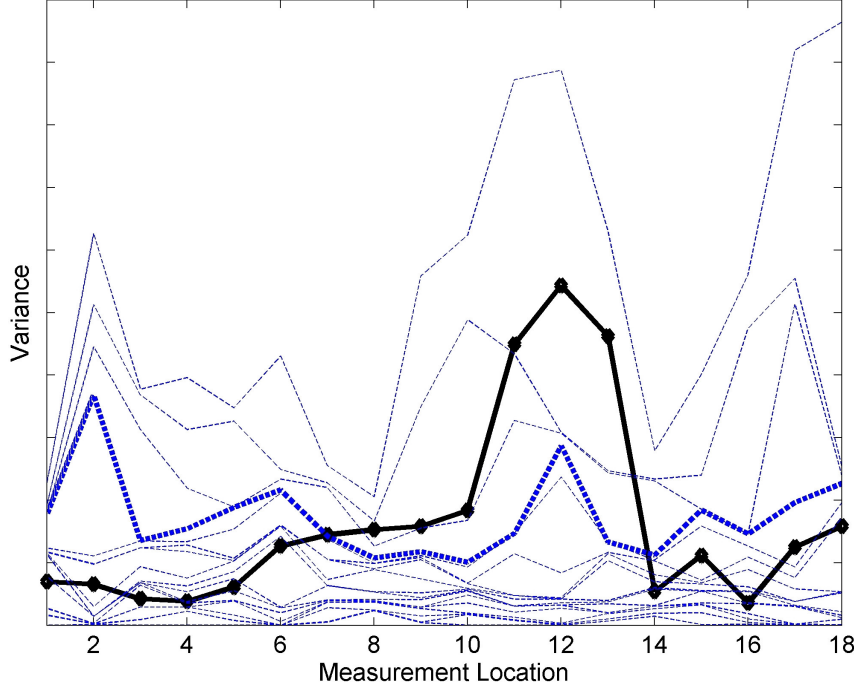


**Fig. 6 Variance vs. measurement location plotted for PCA.**

The expected values of manufactured thicknesses at the 18 measurement positions were then reconstructed using  $d = 4$ . These thickness may be used for lifting, stress or thermal analysis of the probable manufactured blade shapes.

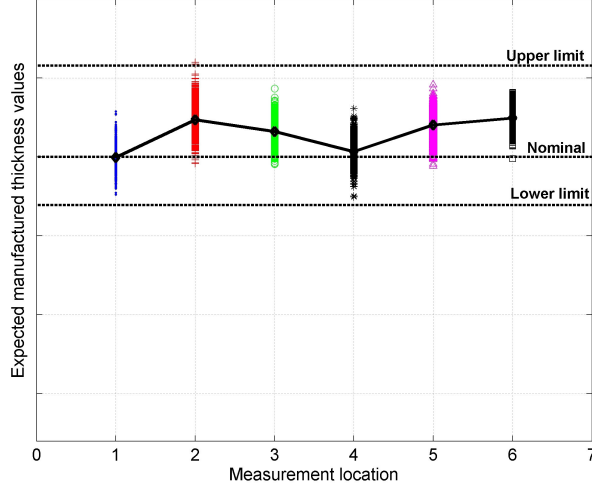


**Fig. 7 Expected manufactured thicknesses vs. measurement location (Tip).**

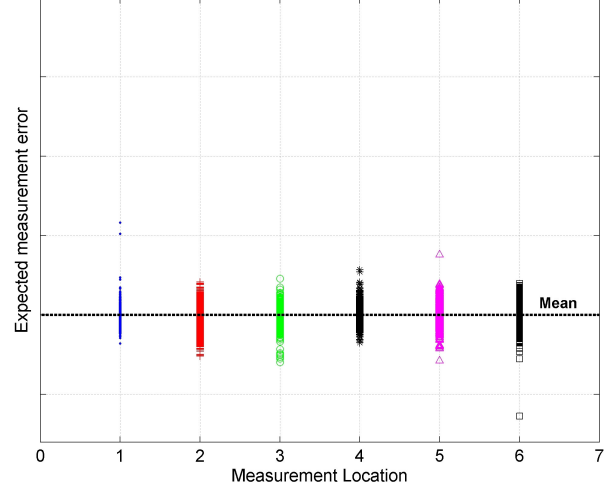


**Fig. 8 Expected measurement error vs. measurement location (Tip).**

The plot obtained for the expected manufactured thicknesses at the Tip-section is shown in **Fig. 7**. **Fig. 8** shows the plot of probable values of measurement error vs. measurement location at Tip-section. Similar plots were also obtained for the Mid and Root-sections. Observing the drift in means from nominal of the expected manufactured thicknesses in **Fig. 7**, it was concluded that the blade thicknesses were influenced by a systematic manufacturing uncertainty. This was also confirmed in the plots obtained for the Mid and Root-sections. Also, it was observed that manufacturing location 1 was most accurate with the mean value of manufactured thicknesses equal to the nominal,

while there was an increase in thicknesses at all the other location number 2-6. The relative increase in thickness seemed to be least at the Root, increased at the Mid-section and was maximum at the Tip of the blade. This increase in wall thickness values from Root to Tip could probably be accounted for by the process in which the molten metal is poured into the casts from base to top, Tip first, followed by Mid and then the Root-section. This is done to ensure that the blade structure is monocrystalline. There is a possibility that the hydrostatic pressure exerted by the high density molten Nickel alloy results in slight increase in the wall thicknesses at the sections located at the bottom of the cast while setting. Also it is highly probable that the ceramic core at such high temperatures of the molten metal becomes semi-plastic in nature, resulting in unexpected deformations in the blade core affecting the wall thicknesses. However, an important point worth noticing is that almost all of the manufactured thickness values are within the specified tolerance limits.

## V. Conclusions

In this paper, we presented an application of PCA in de-noising measurement data on aircraft engine turbine blades. This paper also proposes an approach to dimensionality reduction given prior knowledge of the random error/noise. Comparison of the results obtained from the proposed dimensionality reduction technique with the standard dimensionality reduction techniques proves that for the present case, this approach works successfully in conjunction with PCA for de-noising data. In addition, the variance plot obtained from the repeated measurements while using this approach may provide some extra information on the measurement variability of various measurement types. The values of the manufactured thicknesses obtained from the PCA analysis are representative of the plausible manufactured blade shapes and may be used for life calculations and stress analysis.

From a detailed statistical analysis of the measurements made on a randomly selected sample of 1050 IP turbine blades, we were able to draw the following conclusions:

- The variation in surrounding temperature and humidity levels with passage of time does not appear to affect the relative drifting trends in blade wall thicknesses from design values from one measurement location to another.
- The magnitude of measurement variability is maximum at the Mid-section suction-side center, Mid-section suction-side LE and Root-section pressure-side LE positions possibly due to the large curvature at these positions.
- The measurement variability is lower at the Tip and Root-sections as compared to the Mid-section. A relatively firmer hold on the blade at the Tip and Root-sections due to the presence of shroud and firtree could possibly account for this. It is possible that there is a larger left and right misalignment of the blade at the Mid-section when it is placed perpendicular to the ultrasonic head.
- The magnitude of variance in measurements due to measurement variability is relatively small as compared to the magnitude of the actual wall thickness measurements. This may indicate that the measurement variability being introduced by the operators is relatively small and the operators are well trained.
- Approximately 82% of the variation in the measurement data is captured as manufacturing uncertainty and the remaining 18% variation is filtered out as measurement variability.
- There exists a systematic manufacturing uncertainty in the manufactured turbine blades. The measurements at pressure surface leading edge are most accurate, but all the other measurement locations spread across the pressure and suction surfaces show a slight increase in thickness values from the design values. This relative increase in thicknesses appears to be least at the Root, increases at the Mid-section and is maximum at the Tip of the blade. This variation in thickness could possibly be accounted for by the process in which the molten metal is poured into the casts from base to top to ensure that the blade structure is monocrystalline. There is a possibility that the hydrostatic pressure from the high density molten Nickel alloy, combined with flexibility in the core material at casting temperature, results in slight increase in the wall thicknesses at the sections located at the bottom of the cast while setting.
- Almost all the manufactured thickness values are within the specified tolerance limits.

## Acknowledgements

This work was supported by Rolls-Royce Plc. and the UK DTI.

## References

<sup>1</sup>Moeckel, C.W., "Probabilistic Turbine Blade Thermal Analysis of Manufacturing Variability and Toleranced Designs", in Department of Aeronautics and Astronautics 2006, Massachusetts Institute of Technology.

<sup>2</sup>Royce, R. "Delivering value through services for the 21st century". 2004 [online webpage], URL: <http://www.rolls-royce.com/service/downloads/service.pdf>.

<sup>3</sup>Kumar, A., "Robust Design Methodologies: Application to Compressor Blades", in Faculty of Engineering Sciences and Mathematics, School of Engineering Sciences. 2006, University of Southampton: Southampton.

<sup>4</sup>Tipping, M.E. and C.M. Bishop, "Probabilistic Principal Component Analysis". *Journal of the Royal Statistical Society: Series B (Statistical Methodology)*, 1999. **61**(3): p. 611-622.

<sup>5</sup>Carl, V., E. Becker, and A. Sperling, "Quantitative wall thickness Measurement with Impulse-Video-Thermography", in *7th European Conference on Non-Destructive Testing*. 1998, ECNDT: Copenhagen, Denmark.

<sup>6</sup>Bronnikov, A.V. and D. Killian. "3D Tomography of Turbine Blades". in *International Symposium on Computerized Tomography for Industrial Applications and Image Processing in Radiology* 1999. Berlin, Germany: NDT.net.

<sup>7</sup>Bihan, Y.L., P.Y. Joubert, and D. Placko, "Wall thickness evaluation of single-crystal hollow blades by eddy current sensor". *NDT and E International*, 2001. **34**(5): p. 363 - 368.

<sup>8</sup>Wei, J.J., C.J. Chang, N.K. Chou and G.J. Jan, "ECG Data Compression Using Truncated Singular Value Decomposition". *IEEE Transactions on Information Technology in Biomedicine*, 2001. **5**(4): p. 290 - 299.

<sup>9</sup>Yan, P., S. Wang, and L. Shi, "Electrical Impedance Tomography Based on Sensitivity Theorem with Singular Value Decomposition", in *2005 IEEE Engineering in Medicine and Biology 27th Annual Conference 2005*: Shanghai, China.

<sup>10</sup>Liu, J., S. Chen, and X. Tan, "Fractional order Singular Value Decomposition Representation for Face Recognition". *Pattern Recognition*, 2008. **41**(1): p. 378 - 395.

<sup>11</sup>Smith, L.I. "A tutorial on Principal Components Analysis". 2002 [online database], URL: [http://reflect.otago.ac.nz/cosc453/student\\_tutorials/principal\\_components.pdf](http://reflect.otago.ac.nz/cosc453/student_tutorials/principal_components.pdf).

<sup>12</sup>Wall, M.E., A. Rechtsteiner, and L.M. Rocha, "Singular value decomposition and principal component analysis, in A Practical Approach to Microarray Data Analysis", D.P. Berrar, W. Dubitzky, and M. Granzow, Editors. 2003, Kluwer: Norwell. p. 91-109.

<sup>13</sup>Chiang, K.P. and A. Taniguchi, "Distribution and modification of diatom assemblages in and around a warm core ring in the western North Pacific Frontal Zone east of Hokkaido". *Journal of Plankton Research*, 2000. **22**(11): p. 2061 - 2074.

<sup>14</sup>Ferreira, M.M.C., C.G. Faria, and E.T. Paes, "Oceanographic characterization of northern Sao Paulo Coast: a chemometric study". *Chemometrics and Intelligent Laboratory Systems ELSEVIER*, 1999. **47**(2): p. 289 - 297.

<sup>15</sup>Baeriswyl, P.A. and M. Rebetez, "Regionalization of Precipitation in Switzerland by Means of Principal Component Analysis". *Theoretical and Applied Climatology*, 1997. **58**: p. 31 - 41.

<sup>16</sup>Rabbette, M. and P. Pilewskie. "Principal Component Analysis of Arctic Solar Irradiance Spectra". [online database] URL: <http://geo.arc.nasa.gov/sgp/radiation/rad5.html>.

<sup>17</sup>Hagan, M.E., R.G. Roble, J.M. Russel III and M.G. Mlynaczak, "Complex Principal Component Analysis in the middle Atmosphere : A Feasibility Study using Satellite Sampled Model Data and its Possible Application to Saber Temperatures" in *EGS - AGU - EUG Joint Assembly*. 2003. Nice, France: European Geophysical Society

<sup>18</sup>Rao, N.S., D.J. Devadas, and K.V.S. Rao, "Interpretation of groundwater quality using principal component analysis from Anantapur district, Andhra Pradesh, India". *Environmental Geosciences*, 2006. **13**(4): p. 239 - 259.

<sup>19</sup>Donovan, D.P. and A.I. Carswell, "Principal component analysis applied to multiwavelength lidar aerosol backscatter and extinction measurements". *Applied Optics*, 1997. **36**(36): p. 9406 - 9424.

<sup>20</sup>Klassen, D.R., R.R. Howell, P. Johnson and J.F. Bell, "Principal Components Analysis of Martian Spectral Images", in *28th Annual Meeting of the Division for Planetary Sciences of the American Astronomical Society 1996*: Tucson, Arizona.

<sup>21</sup>Zsemlye, G., "Shape Prediction from Partial Information". 2005, Swiss Federal Institute of Technology: Zurich.

<sup>22</sup>Allen, B., B. Curless, and Z. Popovic, "The space of human body shapes: reconstruction and parameterization from range scans" in *International Conference on Computer Graphics and Interactive Techniques*. 2003, ACM, New York, NY, USA: San Diego, California.

<sup>23</sup>Smidl, V. and A. Quinn, "On Bayesian principal component analysis". *Computational Statistics & Data Analysis* 2007. **51**(9): p. 4101 - 4123.

<sup>24</sup>Shlens, J. "A Tutorial on Principal Component Analysis". 2005 [online database], URL: <http://www.snl.salk.edu/~shlens/pub/notes/pca.pdf>.

<sup>25</sup>Mandel, J., "Use of the Singular Value Decomposition in Regression Analysis". *The American Statistician*, 1982. **36**(1): p. 15 - 24.

<sup>26</sup>Trefethen, L.N. and D. Bau, "Numerical Linear Algebra". 1997, *Society for Industrial and Applied Mathematics*, Philadelphia, PA.

<sup>27</sup>Jolliffe, I.T., *Principal Component Analysis*. 2002, New York: Springer.

<sup>28</sup>Minka, T.P., "Automatic choice of dimensionality for PCA". 2000, MIT Media Laboratory, Vision and Modeling Group, 20 Ames Street: Cambridge, MA 02139.

<sup>29</sup>Wei, H.-L. and S.A. Billings, "Feature Subset Selection and Ranking for Data Dimensionality Reduction". *IEEE Transactions on Pattern Analysis and Machine Intelligence* 2007. **29**(1): p. 162 - 166.

<sup>30</sup>van der Maaten, L.J.P., "An Introduction to Dimensionality Reduction Using Matlab". 2007, Maastricht University: Maastricht, The Netherlands.